Am J Cancer Res 2023;13(8):3449-3462
www.ajcr.us /ISSN:2156-6976/ajcr0151334

Original Article

The application of decision tree model based on clinicopathological risk factors and pre-operative MRI radiomics for predicting short-term recurrence of glioblastoma after total resection: a retrospective cohort study

Peng Du[1,2*], Xuefan Wu[3*], Xiao Liu[4*], Jiawei Chen[5], Lang Chen[2], Aihong Cao[2], Daoying Geng[1]

[1]Department of Radiology, Huashan Hospital, Fudan University, Shanghai 200040, China; [2]Department of Radiology, The Second Affiliated Hospital of Xuzhou Medical University, Xuzhou 221000, Jiangsu, China; [3]Department of Radiology, Shanghai Gamma Hospital, Shanghai 200040, China; [4]School of Computer and Information Technology, Beijing Jiaotong University, Beijing 100044, China; [5]Department of Neurosurgery, Huashan Hospital, Fudan University, Shanghai 200040, China. [*]Equal contributors and co-first authors.

Received May 20, 2023; Accepted July 27, 2023; Epub August 15, 2023; Published August 30, 2023

Abstract: To develop a decision tree model based on clinical information, molecular genetics information and pre-operative magnetic resonance imaging (MRI) radiomics-score (Rad-score) to investigate its predictive value for the risk of recurrence of glioblastoma (GBM) within one year after total resection. Patients with pathologically confirmed GBM at Huashan Hospital, Fudan University between November 2017 and June 2020 were retrospectively analyzed, and the enrolled patients were randomly divided into training and test sets according to the ratio of 3:1. The relevant clinical and MRI data of patients before, after surgery and follow-up were collected, and after feature extraction on preoperative MRI, the LASSO filter was used to filter the features and establish the Rad-score. Using the training set, a decision tree model for predicting recurrence of GBM within one year after total resection was established by the C5.0 algorithm, and scatter plots were generated to evaluate the prediction accuracy of the decision tree during model testing. The prediction performance of the model was also evaluated by calculating area under the receiver operating characteristic (ROC) curve (AUC), ACC, Sensitivity (SEN), Specificity (SPE) and other indicators. Besides, two external validation datasets from Wuhan union hospital and the second affiliated hospital of Xuzhou Medical University were used to verify the reliability and accuracy of the prediction model. According to the inclusion and exclusion criteria, 134 patients with GBM were finally identified for inclusion in the study, and 53 patients recurred within one year after total resection, with a mean recurrence time of 5.6 months. According to the importance of the predictor variables, a decision tree model for predicting recurrence based on five important factors, including patient age, Rad-score, O^6-methylguanine-DNA methyltransferase (MGMT) promoter methylation, pre-operative Karnofsky Performance Status (KPS) and Telomerase reverse transcriptase (TERT) promoter mutation, was developed. The AUCs of the model in the training and test sets were 0.850 and 0.719, respectively, and the scatter plot showed excellent consistency. In addition, the prediction model achieved AUCs of 0.810 and 0.702 in two external validation datasets from Wuhan union hospital and the second affiliated hospital of Xuzhou Medical University, respectively. The decision tree model based on clinicopathological risk factors and preoperative MRI Rad-score can accurately predict the risk of recurrence of GBM within one year after total resection, which can further guide the clinical optimization of patient treatment decisions, as well as refine the clinical management of patients and improve their prognoses to a certain extent.

Keywords: Decision tree model, MRI, radiomics, deep-learning, short-term recurrence, glioblastoma

Introduction

Glioma is the most common primary malignant tumor of the central nervous system (CNS) in adults, originating from glial cells. The annual incidence in China is about 5-8/100000, and the five-year average survival rate is less than 40% [1]. According to the histological malignancy of tumor cells [2], gliomas are classified into: (1) low-grade gliomas (WHO grade 1-2), which

have a high degree of differentiation and a relatively good prognosis; (2) high-grade gliomas (WHO grade 3-4), which are malignant tumors with low differentiation and strong invasion, and have a poor prognosis. Diffuse gliomas in adults are grades 2-4. As the tumor grade increases, the malignancy increases and the prognosis becomes worse. Among adult high-grade gliomas, glioblastoma (GBM) is the most common and has the worst prognosis, with a median survival of only 8 months [3], and relapse eventually occurs regardless of the modality of treatment patients have received [4], so how to optimize treatment and improve prognosis is an urgent clinical problem.

The treatment of GBM is based on surgery, combined with comprehensive treatment methods such as radiotherapy and chemotherapy [5]. Surgery can quickly alleviate the corresponding clinical symptoms of patients and prolong their survival, and the principle is to remove as much of the tumor as possible, which is called safe resection within the maximum extent, while ensuring the safety of patients, protecting neurological functions and important surrounding structures [6]. Although with the deepening of understanding of the genome map and biological behavior of glioma, more and more therapeutic methods have been applied to the clinical treatment of GBM, including targeted therapy, immunotherapy, and electric field therapy, the prognoses of most patients are still not ideal. Studies have shown that the 1-year survival rate of GBM patients is only 40.0%, while the 5-year survival rate is less than 6% [7]. Therefore, it is particularly important to assess the prognosis of patients using existing clinical, pathological, and radiology data, and identify which patients are more likely to relapse in the short term after surgery, requiring more aggressive, even radical and more targeted treatment.

As a form of machine learning, radiomics can transform a large amount of medical image data into data that can be used for mining, to establish and train models, providing clinical decision support and being used for disease diagnosis and prognosis evaluation [8]. Decision tree is a kind of model for decision making based on a tree structure, which is one of the commonly used data mining algorithms. It classifies data sets through several conditional discrimination processes, and finally obtains the required classification results [9]. From a structural perspective, the starting point of the decision tree model is the root node, the intermediate decision-making process is the internal node, and the classification result is the leaf node. Compared with other classification algorithms, decision tree has efficient data mining and processing capability, with the ability to handle both classification and prediction problems at the same time, and the results are highly interpretable and more intuitive [10]. Currently, decision tree models have been widely used in clinical research, including building predictive tools for disease diagnosis or prognosis, identifying and exploring key factors that affect prognoses of diseases, and so on [11-13]. However, few studies have reported the use of decision tree models for predicting short-term recurrence of GBM after total resection, but such predictions may be more meaningful than survival predictions. Mastering the key risk factors that affect recurrence can further guide clinical optimization of patients treatment decisions, while refining patients clinical management, and improving patients prognoses to a certain extent.

In this study, a decision tree model based on basic clinical information, molecular genetics information, pre-operative magnetic resonance imaging (MRI) features and radiomics-score (Rad-score) was developed to investigate its predictive value for the risk of recurrence of GBM within one year after total resection.

Patients and methods

Patients

This study was approved by the institutional review board of Huashan Hospital, Fudan University (Number: KY2021-066). We retrospectively analyzed the data of pathologically confirmed GBM patients at Huashan Hospital, Fudan University from November 2017 to June 2020. Besides, two datasets of GBM patients from Wuhan union hospital and the second affiliated hospital of Xuzhou Medical University were utilized as external validation.

Inclusion and exclusion criteria

Inclusion criteria: (1) patients aged above 18 years; (2) pre-operative Karnofsky Performance

Table 1. Brain MRI scanning parameters

Sequence	Parameters
T1WI	TR = 2992 ms; TI = 869 ms; TE = 24 ms; Matrix = 320 × 320; FOV = 240 × 240 mm^2; Thickness = 5 mm; Interval = 1.5 mm
T2WI	TR = 4599 ms; TE = 102 ms; Matrix = 320 × 224; FOV = 240 × 240 mm^2; Thickness = 5 mm; Interval = 1.5 mm
T2-Flair	TR = 8000 ms; TI = 2100 ms; TE = 160 ms; Matrix = 256 × 256; FOV = 240 × 240 $mm^{2;}$ Thickness = 5 mm; Interval = 1.5 mm
DWI	TR = 4800 ms; TE = 74 ms; Matrix = 128 × 130; FOV = 240 × 240 mm^2; Thickness = 8 mm; Interval = 0.94 mm
CE-T1WI	TR = 2992 ms; TI = 869 ms; TE = 24 ms; Matrix = 320 × 320; FOV = 240 × 240 mm^2; Thickness = 5 mm; Interval = 1.5 mm

Abbreviations: TR = Repetition time; TI = Inversion time; TE = Echo time; FOV = Field of view.

Table 2. Scoring criteria for pre-operative MRI image feature of GBM

MRI image features	Level I (1 point)	Level II (2 points)	Level III (3 points)
Tumor enhancement	Equivalent to or lower than normal brain parenchyma enhancement	Greater than normal brain parenchyma enhancement but weaker than vascular enhancement	Equivalent to or stronger than vascular enhancement
Tumor cystic necrosis	None	Range ≤ 50% of total tumor volume	Range > 50% of total tumor volume
Tumor edema	The distance from the outermost edge of edema to the edge of the tumor < 2 cm	2 cm < distance from the outermost edge of edema to the edge of the tumor < 1/2 of unilateral cerebral hemisphere	Range > 1/2 of unilateral cerebral hemisphere
DWI/ADC	DWI shows equal or low signal; ADC signal does not decrease	DWI shows slightly high signal; ADC signal decreases	DWI shows significant high signal; ADC signal decreases

Abbreviations: DWI = Diffusion weighted imaging; ADC = Apparent diffusion coefficient.

Status (KPS) ≥ 70; (3) patients met the GBM diagnosis of the 2021 WHO CNS tumor classification criteria; (4) the postoperative evaluation of the tumor resection extent was "total resection" (Brain MRI examination was performed within 24-72 hours after surgery, and the enhanced tumor area on contrast enhanced-T1 weighted imaging (CE-T1WI) sequence was completely removed); (5) complete post-operative molecular genetics information (Isocitrate dehydrogenase (IDH) mutation, Telomerase reverse transcriptase (TERT) promoter mutation, O^6-methylguanine-DNA methyltransferase (MGMT) promoter methylation, and 1p/19q co-deletion); (6) standardized radiotherapy and chemotherapy were performed after surgery; (7) brain MRI examination was performed within one week before surgery; (8) complete follow-up brain MRI and clinical information within one year after surgery; (9) brain MRI was acquired using a 3.0T scanner (Discovery MR750W; GE Healthcare, Milwaukee, WI, USA), and the sequences include T1 weighted imaging (T1WI), T2 weighted imaging (T2WI), T2-fluid attenuated inversion recovery (T2-Flair), diffusion weighted imaging (DWI) and CE-T1WI.

Exclusion criteria: (1) previous history of brain tumors; (2) lesion was predominant hemorrhage; (3) artifacts on MRI images; (4) other treatment before surgery; (5) non-recurrent patients followed up for less than one year after surgery; (6) incomplete clinical data.

MRI scanning parameters

Brain MRI scanning parameters are shown in **Table 1**. The scanning range of all sequences covers the entire brain. The contrast agent Gadodiamide injection (GE Pharmaceuticals) is injected through the elbow vein using a dose of 0.1 mmol per kilogram of body weight for CE-T1WI scanning. After the injection of the contrast agent, a transverse CE-T1WI scanning is started immediately, and after the injection of the contrast agent, 20 ml of physiological saline is used to rinse.

Analysis of clinical data and MRI image features

Preoperative data: (1) Basic information of the patient: gender, age, pre-operative KPS, tumor location, and the number of brain lobes involved in the tumor. (2) Preoperative MRI image feature score: tumor enhancement, tumor edema, tumor cystic necrosis, and tumor DWI/ADC signal intensity. The above MRI image features were graded and scored by two radiologists with more than 10 years of experience in neuro-oncology radiology diagnosis (specific scoring criteria are shown in **Table 2**). The comprehensive MRI image feature score (MRI-score) for each patient was obtained by adding the scores.

Postoperative data: (1) Molecular genetics information: IDH mutation, MGMT promoter

Table 3. RANO criteria for evaluation of therapeutic efficacy in gliomas

	CR	PR	SD	PD
CE-T1WI	None	Reduction ≥ 50%	Variation range from -50% ~ +25%	Increase ≥ 25%
T2-Flair	Stable or decreased	Stable or decreased	Stable or decreased	Increased
New lesion	None	None	None	Yes
Hormone use	None	Stable or decreased	Stable or decreased	Not applicable*
Clinical symptoms	Stable or improved	Stable or improved	Stable or improved	Deteriorated
Conditions to be satisfied	All of the above	All of the above	All of the above	Any one of the above

Footnote: *Disease progression is considered to occur when there is a persistent worsening of clinical symptoms, but an increase in hormone dosage should not be used solely as a basis for disease progression. Abbreviations: CR = Complete response; PR = Partial response; SD = Stable disease; PD = Progressive disease.

methylation, 1p/19q co-deletion, and TERT promoter mutation. (2) Start time of radiotherapy: All patients received three-dimensional conformal radiotherapy after surgery, with a conventional fractionation and a total radiation dose in the range of 54-60 Gy. The starting time of post-operative radiotherapy was divided into early (within 2-6 weeks after surgery) and non-early (beyond 6 weeks after surgery). (3) Temozolomide (TMZ) adjuvant chemotherapy cycle: All patients received radiotherapy and concurrent TMZ chemotherapy, and then continued to use the TMZ adjuvant chemotherapy regimen. During radiotherapy, TMZ was administered orally at a dose of 75 mg/(m^2·d) for 42 consecutive days. Four weeks after the end of concurrent radiotherapy and chemotherapy, adjuvant chemotherapy was administered with an oral TMZ dose of 150-200/(m^2·d) for 5 consecutive days, with a chemotherapy cycle of every 28 days. TMZ adjuvant chemotherapy cycle was divided into standard cycle (6 cycles) and extended cycle (> 6 cycles).

Evaluation of postoperative recurrence: Postoperative recurrence was determined by a multidisciplinary team of experts including neurosurgery, radiology, radiotherapy, neuro-oncology, pathology, and neurology based on the follow-up MRI images and clinical manifestations of patients after surgery, with reference to the "Guidelines for the Diagnosis and Treatment of Gliomas in China (2022 Edition)". This guideline stipulates that the brain MRI (plain scan and contrast enhancement) within 24-72 hours after surgery should be used as the baseline radiology data, and the RANO standard [14] should be used as the evaluation standard for treatment efficacy, which is shown in **Table 3**. Besides, perfusion weighted imaging (PWI), the ratio of choline (Cho)/N-acetylaspartate (NAA) and Cho/creatine (Cr) in magnetic resonance spectroscopy (MRS) should be used as the basis for distinguishing tumor recurrence, pseudo-progression, and radiation necrosis.

MRI data pre-processing: First, we performed an anonymous operation on the image information of all patients included in the study. Then, in order to match the region of interest (ROI) with the images of all MRI sequences, we used the linear differential resampling method in SimpleITk software package (version 2.1.1.1, https://simpleitk.readthedocs.io/en/master/index.html), resampling all images to 240 × 240 × 24 with interval of 1 × 1 × 4 mm^3. After that, by using Advanced Normalization Tools (ANTs) (https://github.com/ANTsX), all MRI sequences (T1WI, T2WI, T2-Flair, and DWI) were registered to CE-T1WI sequence. Then, we utilized the feature scaling method provided in SimpleITK to normalize the image grayscale value to 0-255.

MRI image segmentation: The MRI image segmentation of tumors was based on the expert consensus on MRI image labeling of CNS tumors released in China in 2021, and the judgment of glioma components was based on the research of Zacharaki et al. [15]. MRI image segmentation of all tumors was performed by a radiologist with more than 10 years of experience in neuro-oncology radiology diagnosis. The tumors were segmented on T2-Flair and CE-T1WI axial images, using the semi-automatic tool ITK-SNAP (version 4.0.0, http://www.itksnap.org/pmwiki/pmwiki.php). All tumors were delineated in two parts, named ROI1 and ROI2: (1) ROI1 represented the maximum anomaly region of the tumor, including the tumor body and peri-tumoral edema. It was delineated on the T2-Flair image as an area displaying abnormal high signal, represented in green; (2) ROI2 represented the tumor area, which was delineated on the CE-T1WI image, with yellow representing the tumor enhancement area and red representing the non-enhancement area of the

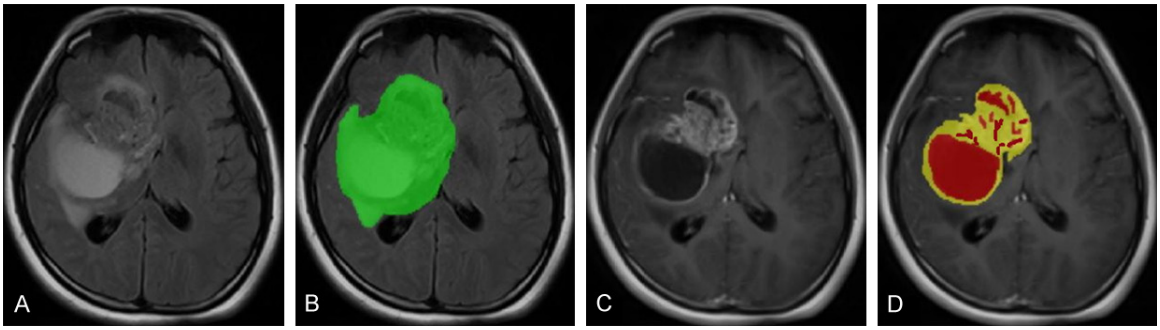

Figure 1. A case of WHO grade 4 glioblastoma, (A, B) are T2-Flair images, and (C, D) are CE-T1WI images. (B) Represents the maximum anomaly region of the tumor delineated in green. (D) Represents the tumor region, yellow represents the enhancement region of tumor, and red represents the non-enhancement region of tumor.

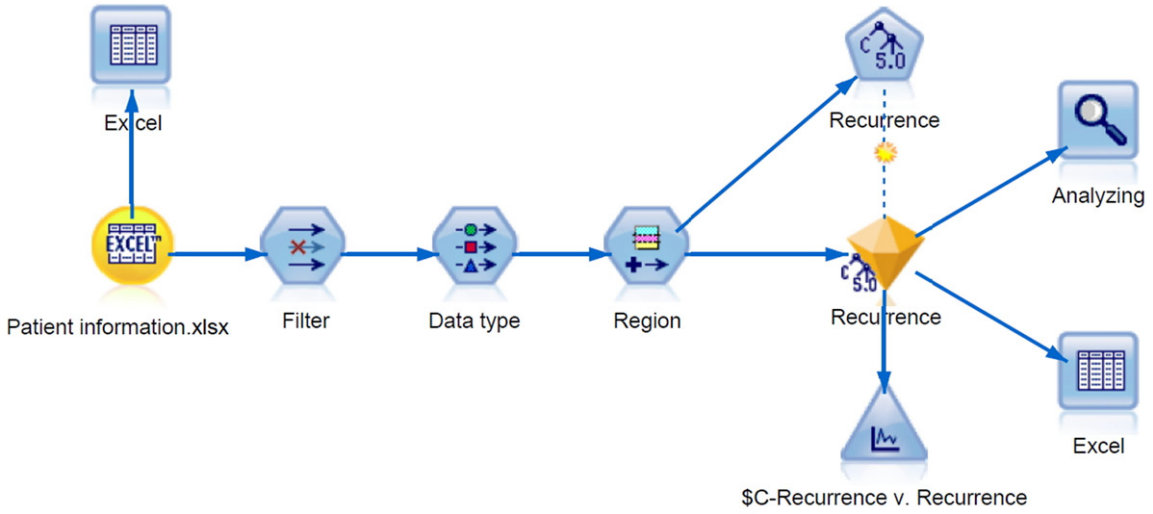

Figure 2. The analysis stream of decision tree development and validation, including processes of data input, data filtrating, data type determination, model training, and model testing.

tumor. The above two parts of segmentation required simultaneous reference to all MRI sequences. A representative tumor ROI delineation is shown in **Figure 1**.

Radiomics feature extraction and selection

The PyRadiomics (Version 3.0, https://pyradiomics.readthedocs.io/en/latest/features.html) was used to force extraction of two-dimensional features, using slice average features instead of three-dimensional features, and a total of 4306 features were extracted. Then, least absolute shrinkage and selection operator (LASSO) filter was utilized to filter the features and establish the Rad-score.

Decision tree model establishment

All enrolled patients were randomly divided into training and test sets, with a ratio of 3:1. Using the training set, a decision tree model was established utilizing C5.0 algorithm, and the depth of the decision tree was limited to 5 layers. The process of establishing and verifying the decision tree model is shown in **Figure 2**, including data input, data filtering, data type determination, model training, and model testing. During model testing, a scatter chart was generated to evaluate the prediction accuracy of the decision tree.

Decision tree model evaluation and statistical methods

The prediction performance of the decision tree model was evaluated by calculating area under the receiver operating characteristic (ROC) curve (AUC), sensitivity (SEN), specificity (SPE), positive prediction value (PPV), negative prediction value (NPV), accuracy (ACC), false

positive rate (FPR), false negative rate (FNR), and Youden's index (YI).

All statistical analyses were conducted using R software version 4.1.3 and SPSS Modeler 18.0.

Results

Baseline characteristics

According to the inclusion criteria, a total of 192 patients were recruited for this study, and 58 patients were excluded: 6 cases had a history of brain tumor in the past; 5 cases had lesions with predominant hemorrhage; 12 cases had artifacts on MRI images; 9 cases had received treatment before surgery; 15 cases had no recurrence after a follow-up of less than one year; 11 cases had incomplete clinical data. Finally, 134 GBM patients with IDH wild-type were identified for inclusion in the study, and the training set and test sets were divided randomly with a ratio of 3:1.

The basic clinical information, molecular genetics information, and pre-operative MRI image feature score of 134 GBM patients are shown in **Table 4**. There were 53 cases of recurrence within 1 year after surgery, including 34 males and 19 females, and the average recurrence time was 5.6 months. The MRI manifestations of tumor recurrence were diverse, presenting as mass type, nodular type, diffuse type, or marginal type. The vast majority of tumor recurrences occurred within the original surgical area, while only 3 cases had distant recurrences (more than 3 cm from the edge of the surgical area).

In addition, basing on the inclusion and exclusion criteria, 37 GBM patients from Wuhan union hospital and 26 GBM patients from the second affiliated hospital of Xuzhou Medical University were enrolled as the external validation datasets.

Rad-score establishment

LASSO filter was utilized to filter 4306 MRI radiomics features extracted from CE-T1WI sequence, and ultimately 12 optimal features were retained, including gray level co-occurrence matrix (glcm) feature (n = 4), gray level dependency matrix (gldm) feature (n = 1), gray level run length matrix (glrlm) feature (n = 3), gray level size zone matrix (glszm) feature (n = 3), and neighboring gray tone difference matrix (ngtdm) feature (n = 1). According to the regional distribution, 6 features came from the maximum anomaly region, and 6 features came from the tumor region. The Rad-score formula established based on optimal characteristics is shown in **Table 5**, and the Rad-score distribution is shown in **Figure 3**. The average Rad-score for recurrent patients was 0.64 ± 0.05, and the average Rad-score for non-recurrent patients was 0.49 ± 0.07. There was a significant statistical difference between the two groups (two independent sample T test, t = 8.458, $P < 0.001$***), which indicated that the Rad-score established based on the 12 optimal features can predict the stratification of recurrence outcomes of GBM within one year after total resection.

Establishment and validation of decision tree model

The order of importance of the predictive variables for each decision tree is shown in **Figure 4**. Patient age, Rad-score, MGMT promoter methylation, pre-operative KPS, and TERT promoter mutation were important for predicting recurrence in GBM patients within one year after total resection. Based on these predictive variables, a decision tree model for recurrence of GBM patients within one year after total resection was generated, as shown in **Figure 5**.

Figure 6 shows a scatter plot (including training and test sets) that evaluates the consistency between predicted and actual recurrence. There is good consistency between the predicted recurrence and actual recurrence status of the two sets. Most of the scatter points are located on the diagonal line, and the fitting line is near the asymptotic line of "y = x", showing excellent consistency.

The prediction performance indicators of the decision tree model are shown in **Table 6**, and the ROC curve is shown in **Figure 7**. The model achieved AUC: 0.850, ACC: 0.898, SEN: 0.816, SPE: 0.950 in the training set, and AUC: 0.719, ACC: 0.833, SEN: 0.867, SPE: 0.810 in the test set, respectively. The above results show that the decision tree model has good prediction performance.

In external validation, the prediction model achieved an AUC of 0.810, an ACC of 0.811, a SEN of 0.810, a SPE of 0.813 based on the

Table 4. Baseline characteristics of the enrolled patients

Characteristics	Overall (N = 134)	Training set (N = 98)	Testing set (N = 36)
Gender			
Male	83 (62%)	58 (59%)	25 (69%)
Female	51 (38%)	40 (41%)	11 (31%)
Age (years)			
< 50	56 (42%)	41 (42%)	15 (42%)
≥ 50	78 (58%)	57 (58%)	21 (58%)
KPS			
≤ 80	76 (57%)	57 (58%)	19 (53%)
> 80	58 (43%)	41 (42%)	17 (47%)
Location			
Frontal lobe	72 (54%)	56 (57%)	16 (44%)
Temporal lobe	27 (20%)	21 (21%)	6 (17%)
Parietal lobe	14 (10%)	9 (9%)	5 (14%)
Insular lobe	8 (6%)	5 (5%)	3 (8%)
Occipital lobe	5 (4%)	4 (4%)	1 (3%)
Others	8 (6%)	3 (3%)	5 (14%)
Hemisphere			
Left	84 (63%)	54 (55%)	30 (83%)
Right	50 (37%)	44 (45%)	6 (17%)
Lobe involvement			
Single	111 (83%)	81 (83%)	30 (83%)
Multiple	23 (17%)	17 (17%)	6 (17%)
MRI-score			
< 9	50 (37%)	39 (40%)	11 (31%)
≥ 9	84 (63%)	59 (60%)	25 (69%)
MGMT promoter methylation			
Yes	61 (46%)	45 (46%)	16 (44%)
No	73 (54%)	53 (54%)	20 (56%)
1p/19q co-deletion			
Yes	20 (15%)	11 (11%)	9 (25%)
No	114 (85%)	87 (89%)	27 (75%)
TERT promoter mutation			
Yes	60 (45%)	44 (45%)	16 (44%)
No	74 (55%)	54 (55%)	20 (56%)
Start time of postoperative radiotherapy			
Early	71 (53%)	51 (52%)	20 (56%)
Non-early	63 (47%)	47 (48%)	16 (44%)
TMZ adjuvant chemotherapy cycle			
Standard	69 (52%)	49 (50%)	20 (56%)
Extended	65 (48%)	49 (50%)	16 (44%)

Abbreviations: KPS = Karnofsky Performance Status; MRI-score = Magnetic resonance imaging-score; MGMT = O^6-methylguanine-DNA methyltransferase; 1p = The short arm of chromosome 1; 19q = The long arm of chromosome 19; TERT = Telomerase reverse transcriptase; TMZ = Temozolomide.

dataset from Wuhan union hospital; the prediction model achieved an AUC of 0.702, an ACC of 0.808, a SEN of 0.786, a SPE of 0.833 based on the dataset from the second affiliated hospital of Xuzhou Medical University.

Discussion

GBM is the most common primary malignant brain tumor in adults, accounting for more than half of all gliomas [16]. Currently, the treatment

Table 5. Rad-score formula

Rad-score = 0.32013 × log-sigma-4-mm-3D_glszm_LowGrayLevelZoneEmphasis_CE-T1WI_MAR + 0.25611 × wavelet-HH_gldm_DependenceEntropy_CE-T1WI_MAR + 0.20272 × exponential_glcm_Imc1_CE-T1WI_Tumor + 0.07867 × square_ngtdm_Coarseness_CE-T1WI_MAR + 0.07621 × exponential_glcm_Imc2_CE-T1WI_Tumor + 0.0724 × squareroot_glcm_ClusterProminence_CE-T1WI_Tumor + 0.03685 × log-sigma-4-mm-3D_glrlm_ShortRunHighGrayLevelEmphasis_CE-T1WI_Tumor + 0.02929 × logarithm_glcm_Correlation_CE-T1WI_Tumor + 0.02244 × log-sigma-3-mm-3D_glrlm_LongRunLowGrayLevelEmphasis_CE-T1WI_MAR + 0.0206 × squareroot_glszm_SmallAreaEmphasis_CE-T1WI_MAR + 0.01341 × log-sigma-5-mm-3D_glszm_LowGrayLevelZoneEmphasis_CE-T1WI_Tumor + 0.01032 × log-sigma-4-mm-3D_glrlm_LongRunLowGrayLevelEmphasis_CE-T1WI_MAR

Abbreviations: glszm = Gray Level Size Zone Matrix; CE-T1WI = Contrast enhanced-T1 weighted imaging; MAR = Maximum anomaly region; gldm = Gray level dependence matrix; glcm = Gray level co-occurrence matrix; ngtdm = Neighboring gray tone difference matrix; glrlm = Gray level run length matrix.

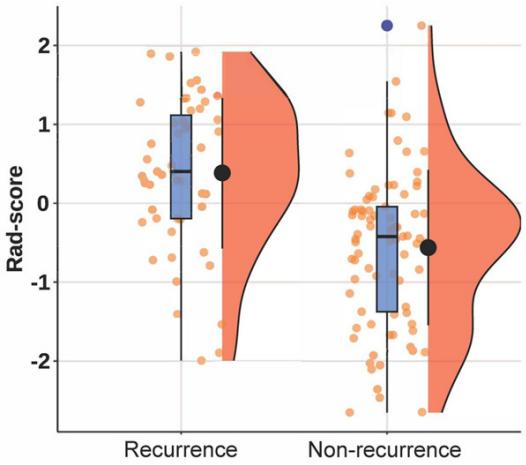

Figure 3. Rad-score distribution in GBM patients with and without recurrence.

of GBM is based on surgery within the maximum extent of safe resection, supplemented by postoperative radiotherapy and chemotherapy. However, the prognosis of patients is still poor. According to incomplete statistics, the 1-year survival rate of GBM patients is only 40.0%, while the 5-year survival rate is less than 6% [17]. In recent years, in order to further improve the survival rate and prognosis of patients, a large number of basic experiments and clinical studies on GBM have been carried out worldwide, and human understanding of the genome map and biological behavior of GBM has gradually deepened. At the same time, the continuous development and widespread application of new micro-surgical techniques have improved the total resection rate of GBM to a certain extent [18]. In addition, the application of new therapeutic methods, including targeted therapy, immunotherapy, and electric field therapy, in GBM treatment has also achieved certain results [19, 20].

Therefore, it is particularly important to assess the prognosis of patients using existing clinical, pathological, and radiology data, and identify which patients are more likely to relapse in the short term after surgery, requiring more aggressive, even radical and more targeted treatment. By integrating the basic clinical information, molecular genetics information, pre-operative MRI image features and Rad-score of GBM patients, and analyzing the importance of predictive variables, we find that age, pre-operative KPS, Rad-score, MGMT promoter methylation, and TERT promoter mutation are important predictive factors for recurrence within 1 year after total resection in GBM patients. Combining the above predictive factors, a decision tree model is established, trained and tested. The model achieves AUC: 0.850 in the training set and AUC: 0.719 in the test set.

Many studies have shown that although the prognosis of GBM patients is generally poor, the prognosis of elderly patients is significantly worse than that of young patients, and their median survival period is shorter [21]. With the increasing degree of population aging, the incidence rate of GBM in elderly patients is rising [22]. Compared with young patients, older patients are more likely to suffer from chronic diseases such as diabetes and hypertension, and their immunity and metabolic function will also decline accordingly. Their tolerance to treatment is relatively poor, including trauma caused by surgery and adverse reactions caused by post-operative radiotherapy and chemotherapy. Babu et al. [23] conducted a retrospective study of 120 newly diagnosed GBM patients between 2004 and 2010, and found that age was an important prognostic factor. Luo et al. [24] supposed that indicators such as age < 55 years old, IDH mutation, and total tumor resection suggested a good prognosis for GBM patients. The research by Zhang et al. [25] indicated that older age, IDH wide-type, and lower degree of tumor resection were independent predictors of shorter survival in GBM patients.

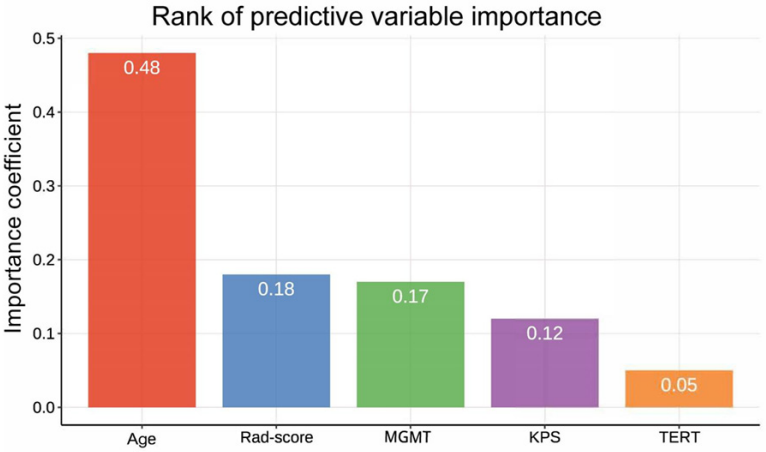

Figure 4. The rank of predictive variable importance of decision tree model. MGMT represents MGMT promoter methylation; TERT represents TERT promoter mutation.

According to the statistical report from the Central Brain Tumor Registry of United States (CBTRUS) [16], GBM is more common in men. In this study, there were 83 male and 51 female patients. No significant correlation was found between gender and recurrence within 1 year after surgery. Carson et al. [26] opined that gender and ethnicity cannot be used as indicators of prognosis in patients with glioma. However, Patil et al. [27] analyzed the data from two clinical trials, NRG/RTOG 0525 and NRG/RTOG 0825, and found that women with GBM had a longer median survival and overall survival (OS) than men. We believe that the correlation between gender and GBM prognosis is uncertain, and prospective, multi-centered, and larger clinical trials are needed to evaluate it. KPS is a universal quality of life evaluation standard for cancer patients, originally used to assess whether cancer patients can tolerate chemotherapy. The higher the score, the better the patient's physical condition, and more conducive to tolerating the side effects caused by tumor treatment [28]. Several studies [25, 27] showed that GBM patients with KPS above 80 had better post-operative status and longer survival time, which is basically consistent with the results of this study.

The MRI manifestations of glioma reflect the tumor's cellular heterogeneity, neovascularization, destruction of the blood brain barrier, and infiltration of surrounding tissues [29]. In this study, the mean MRI-score of 134 GBM patients is 9 points, and the mean MRI-score of 53 patients with recurrence within 1 year after surgery is also 9 points. No correlation between MRI-score and short-term recurrence is found. Romano et al. [30] found that the minimum ADC value in the enhanced portion of GBM tumors was related to the patient's progression free survival (PFS) and OS, and patients with significantly reduced ADC values had a poor prognosis. Pérez-Beteta et al. [31] opined that the tumor necrosis area of GBM was significantly related to the poor prognosis of patients. We believe that MRI is one of the important methods for the diagnosis and differential diagnosis of glioma, and the MRI-score based on MRI features in this study achieved quantitative evaluation of tumors to a certain extent, but lacked objectivity, so further use of other objective means to quantitatively evaluate MRI image features is needed.

The MGMT promoter methylation status, which regulates MGMT gene expression, is considered a biological marker for predicting GBM prognosis and TMZ chemotherapy sensitivity. However, some studies have also found inconsistency between MGMT promoter methylation and protein expression [32]. It has been reported [33] that low expression of MGMT protein or mRNA was positively associated with improved patient survival and outcome, but MGMT promoter methylation was not. Several studies have shown that MGMT promoter methylation was associated with better prognoses for GBM patients. In this study, we find that MGMT promoter methylation and recurrence within 1 year after total resection in GBM patients are negatively correlated. Therefore, we believe that MGMT has some application in the treatment decision and prognosis assessment of GBM patients.

TERT promoter mutation is a marker for better prognoses in IDH mutant gliomas, while suggesting worse prognoses in IDH wild-type gliomas [34]. In a study of 473 adult gliomas, Killera et al. [35] found that patients carrying both TERT promoter mutation and IDH wild-

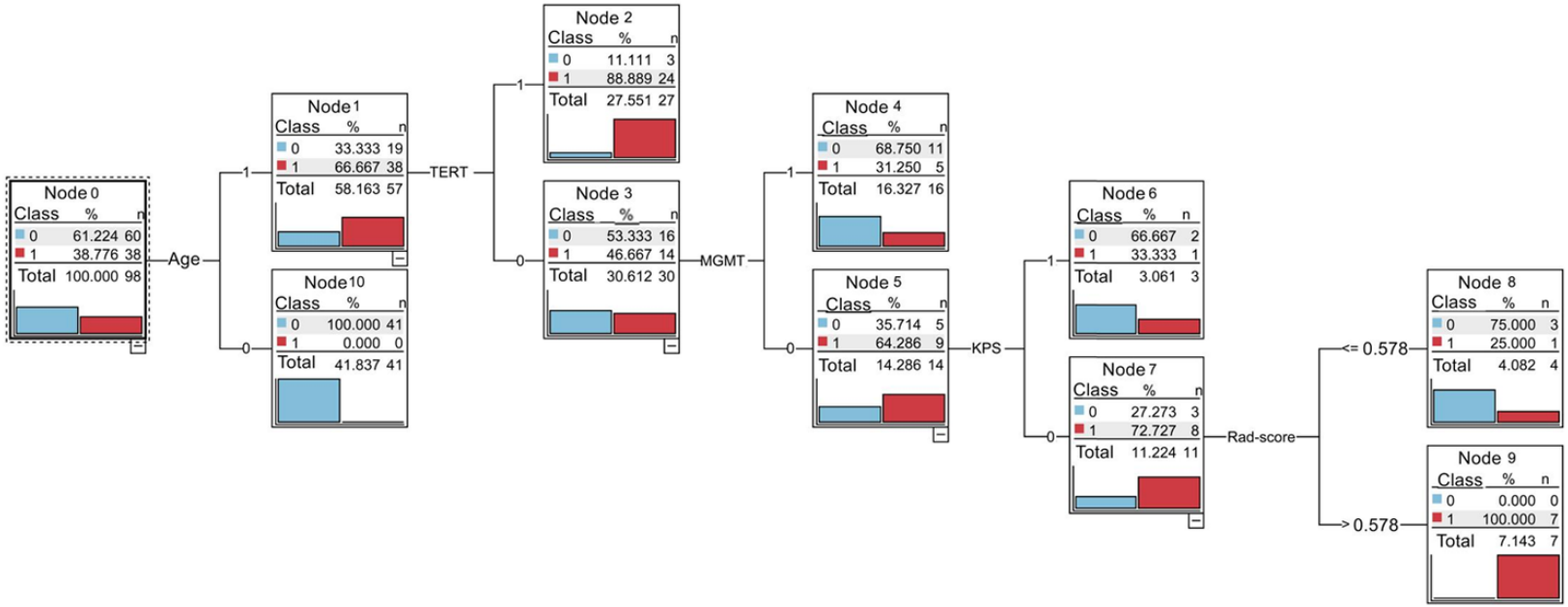

Figure 5. A decision tree model for GBM patients with recurrence within one year after total resection was established using the C5.0 algorithm. Patient age, Rad-score, MGMT promoter methylation, pre-operative KPS, and TERT promoter mutation are of great significance in predicting recurrence within one year after total resection in GBM patients; Age-1 represents ≥ 50 years old and 0 represents < 50 years old; TERT-1 represents TERT promoter mutation and 0 represents no mutation; MGMT-1 represents MGMT promoter methylation and 0 represents un-methylation; KPS-1 represents > 80 and 0 represents ≤ 80; The optimal cutoff value for Rad-score is 0.578.

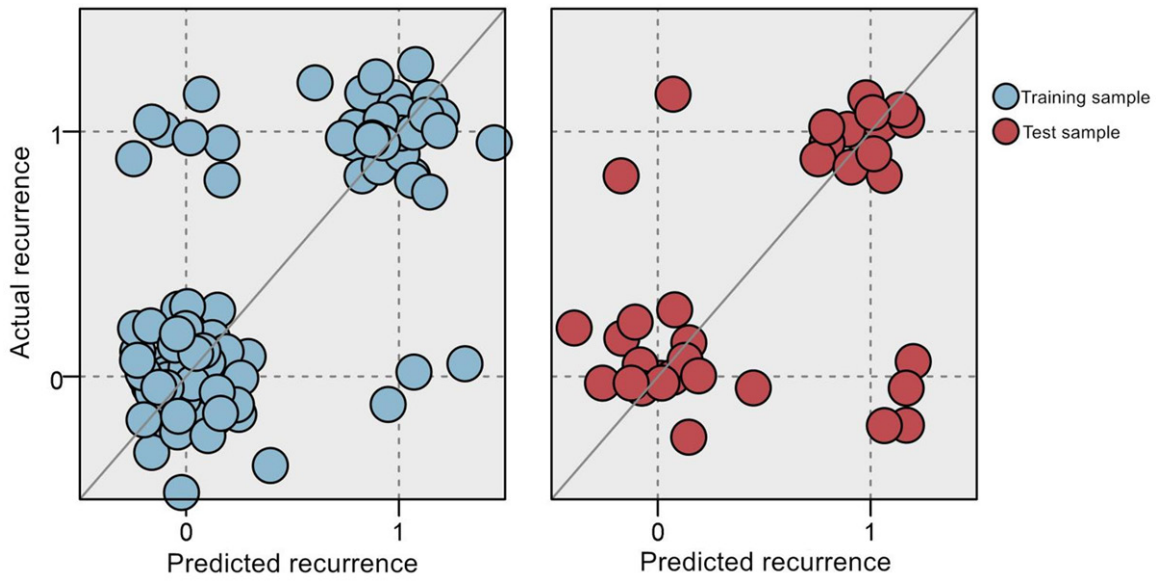

Figure 6. A scatter plot (including training and test sets) that evaluates the consistency between predicted and actual recurrence. There is good consistency between the predicted recurrence and actual recurrence status of the two sets. Most of the scatter points are located on the diagonal line, and the fitting line is near the asymptotic line of "y = x", showing good consistency.

Table 6. Prediction performance indicators of decision tree model

Indicator	AUC	ACC	SEN	SPE	PPV	NPV	FPR	FNR	YI
Training set	0.850	0.898	0.816	0.950	0.912	0.891	0.050	0.184	0.766
Test set	0.719	0.833	0.867	0.810	0.765	0.895	0.191	0.133	0.676

Abbreviations: AUC = Area under curve; ACC = Accuracy; SEN = Sensitivity; SPE = Specificity; PPV = Positive prediction value; NPV = Negative prediction value; FPR = False positive rate; FNR = False negative rate; YI = Youden's index.

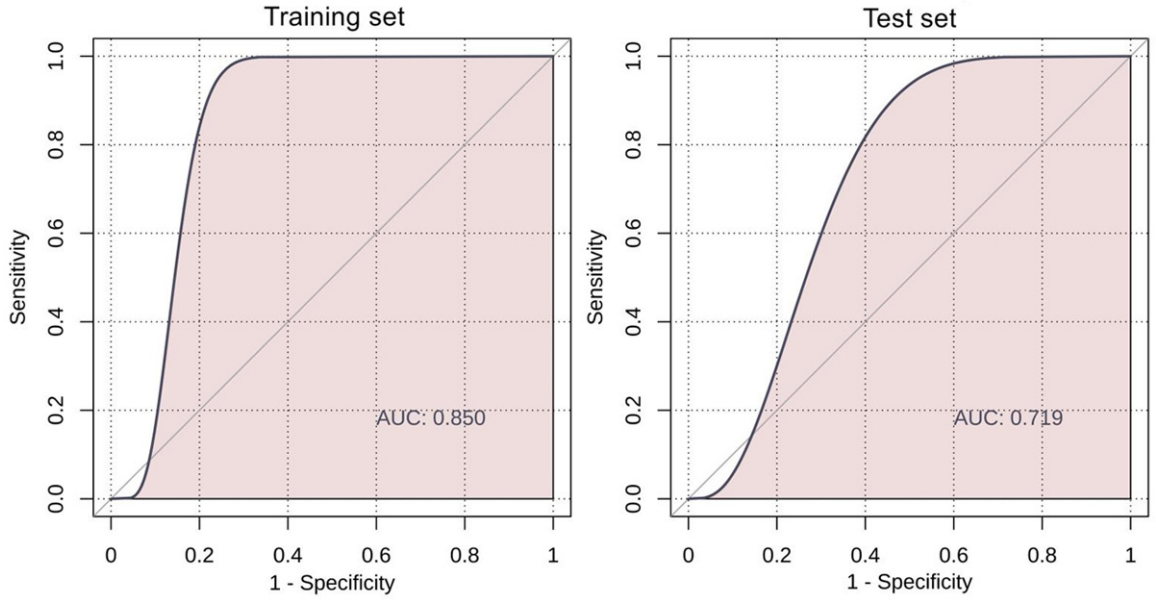

Figure 7. ROC curves of decision tree model in training and test sets.

type had the shortest OS. Similarly, the study by Labuissère et al. [36] suggested that in GBM patients, the presence of TERT promoter mutation was an independent factor for poor prog-

nosis. In this study, TERT promoter mutation is found to be positively associated with patient recurrence within 1 year after surgery, which is generally consistent with the findings in the literature.

It has been shown [37] that in newly diagnosed GBM patients, a modest delay in starting postoperative radiotherapy and chemotherapy did not appear to be associated with poorer PFS or OS, whereas a significant delay of more than 6 weeks may be associated with poorer OS. Zhang et al. [38] retrospectively analyzed the data of 66 patients with GBM and found that the start of postoperative adjuvant radiotherapy that exceeded 6 weeks led to a decrease in survival, and therefore recommended that postoperative adjuvant radiotherapy be initiated within 6 weeks post-operatively. However, it has also been suggested [39] that extending the time to start postoperative radiotherapy to 50 days had no effect on OS or PFS. We believe that the inherent limitations of retrospective studies and the insufficient number of patients enrolled may have contributed to the discrepancy in the results of the above studies. This study does not find a significant correlation between the time of initiation of postoperative radiotherapy and recurrence outcome.

Radiomics features refer to high-throughput quantitative features extracted from medical images, which cannot be recognized by the naked eye and may be related to genetic features [8]. From the importance analysis of predictive variables, it can be clearly seen that the predictive importance of Rad-score is inferior to age, ranking second among the five important factors, indicating that the Radiomics features have significant predictive significance for the prognosis of GBM patients. Compared to other data mining algorithms, the decision tree model does not need to make any assumptions about the structure and distribution of data, with decision-making process closer to human thinking. Besides, it is very intuitive and easy to interpret. The decision tree model based on multiple factors established in this study can effectively predict the recurrence of GBM patients within one year after total resection, which is conducive to further optimizing clinical treatment decisions and refining clinical management of patients.

However, our study still has some inevitable limitations. Firstly, this study is a single center retrospective study with a small sample size, which inevitably leads to bias. We need to conduct larger, prospective, and multi-centered study in future to further verify the predictive performance of the model. Secondly, radiation dose, radiation energy, and the mechanism of action between radiation therapy and biological individuals are extremely complex, with a large number of uncontrollable factors and individual biological randomness, which may affect the prognosis of patients. We have not discussed them here and need to pay attention to them in future research.

Conclusions

The decision tree model based on clinicopathological risk factors and preoperative MRI Rad-score established in this study can accurately predict the risk of recurrence within one year of GBM after total resection, which can further guide clinical optimization of patient treatment decisions, while refining patient clinical management, and improving patient prognosis to a certain extent.

Acknowledgements

This work was supported by Greater Bay Area Institute of Precision Medicine (Guangzhou), Fudan University (21618), and Science and Technology Commission of Shanghai Municipality (22TS1400900).

A waiver for informed consent was issued given that this study used data collected as part of the participants' routine care.

Disclosure of conflict of interest

None.

Address correspondence to: Aihong Cao, Department of Radiology, The Second Affiliated Hospital of Xuzhou Medical University, No. 32, Meijian Road, Xuzhou 221000, Jiangsu, China. E-mail: caoaihong0516@126.com; Daoying Geng, Department of Radiology, Huashan Hospital, Fudan University, 12 Wulumuqi Middle Road, Shanghai 200040, China. E-mail: gdy_2019@163.com

References

[1] Zhang K, Liu X, Li G, Chang X, Li S, Chen J, Zhao Z, Wang J, Jiang T and Chai R. Clinical management and survival outcomes of patients with different molecular subtypes of dif-

fuse gliomas in China (2011-2017): a multicenter retrospective study from CGGA. Cancer Biol Med 2022; 19: 1460-1476.
[2] Louis DN, Perry A, Wesseling P, Brat DJ, Cree IA, Figarella-Branger D, Hawkins C, Ng HK, Pfister SM, Reifenberger G, Soffietti R, von Deimling A and Ellison DW. The 2021 WHO classification of tumors of the central nervous system: a summary. Neuro Oncol 2021; 23: 1231-1251.
[3] Omuro A and DeAngelis LM. Glioblastoma and other malignant gliomas: a clinical review. JAMA 2013; 310: 1842-1850.
[4] Alexander BM and Cloughesy TF. Adult Glioblastoma. J Clin Oncol 2017; 35: 2402-2409.
[5] De Biase G, Garcia DP, Bohnen A and Quiñones-Hinojosa A. Perioperative management of patients with glioblastoma. Neurosurg Clin N Am 2021; 32: 1-8.
[6] Karschnia P, Vogelbaum MA, van den Bent M, Cahill DP, Bello L, Narita Y, Berger MS, Weller M and Tonn JC. Evidence-based recommendations on categories for extent of resection in diffuse glioma. Eur J Cancer 2021; 149: 23-33.
[7] Brown TJ, Brennan MC, Li M, Church EW, Brandmeir NJ, Rakszawski KL, Patel AS, Rizk EB, Suki D, Sawaya R and Glantz M. Association of the extent of resection with survival in glioblastoma: a systematic review and meta-analysis. JAMA Oncol 2016; 2: 1460-1469.
[8] Gillies RJ, Kinahan PE and Hricak H. Radiomics: images are more than pictures, they are data. Radiology 2016; 278: 563-577.
[9] Flayer CH, Perner C and Sokol CL. A decision tree model for neuroimmune guidance of allergic immunity. Immunol Cell Biol 2021; 99: 936-948.
[10] Al Fryan LH, Shomo MI, Alazzam MB and Rahman MA. Processing decision tree data using internet of things (IoT) and artificial intelligence technologies with special reference to medical application. Biomed Res Int 2022; 2022: 8626234.
[11] Brims FJ, Meniawy TM, Duffus I, de Fonseka D, Segal A, Creaney J, Maskell N, Lake RA, de Klerk N and Nowak AK. A novel clinical prediction model for prognosis in malignant pleural mesothelioma using decision tree analysis. J Thorac Oncol 2016; 11: 573-582.
[12] Hostettler IC, Muroi C, Richter JK, Schmid J, Neidert MC, Seule M, Boss O, Pangalu A, Germans MR and Keller E. Decision tree analysis in subarachnoid hemorrhage: prediction of outcome parameters during the course of aneurysmal subarachnoid hemorrhage using decision tree analysis. J Neurosurg 2018; 129: 1499-1510.
[13] Lorenzo D, Ochoa M, Piulats JM, Gutiérrez C, Arias L, Català J, Grau M, Peñafiel J, Cobos E, Garcia-Bru P, Rubio MJ, Padrón-Pérez N, Dias B, Pera J and Caminal JM. Prognostic factors and decision tree for long-term survival in metastatic uveal melanoma. Cancer Res Treat 2018; 50: 1130-1139.
[14] Wen PY, Macdonald DR, Reardon DA, Cloughesy TF, Sorensen AG, Galanis E, Degroot J, Wick W, Gilbert MR, Lassman AB, Tsien C, Mikkelsen T, Wong ET, Chamberlain MC, Stupp R, Lamborn KR, Vogelbaum MA, van den Bent MJ and Chang SM. Updated response assessment criteria for high-grade gliomas: response assessment in neuro-oncology working group. J Clin Oncol 2010; 28: 1963-1972.
[15] Zacharaki EI, Wang S, Chawla S, Soo Yoo D, Wolf R, Melhem ER and Davatzikos C. Classification of brain tumor type and grade using MRI texture and shape in a machine learning scheme. Magn Reson Med 2009; 62: 1609-1618.
[16] Ostrom QT, Gittleman H, Truitt G, Boscia A, Kruchko C and Barnholtz-Sloan JS. CBTRUS statistical report: primary brain and other central nervous system tumors diagnosed in the United States in 2011-2015. Neuro Oncol 2018; 20: iv1-iv86.
[17] Cheng JX, Zhang X and Liu BL. Health-related quality of life in patients with high-grade glioma. Neuro Oncol 2009; 11: 41-50.
[18] Verburg N and de Witt Hamer PC. State-of-the-art imaging for glioma surgery. Neurosurg Rev 2021; 44: 1331-1343.
[19] Yang K, Wu Z, Zhang H, Zhang N, Wu W, Wang Z, Dai Z, Zhang X, Zhang L, Peng Y, Ye W, Zeng W, Liu Z and Cheng Q. Glioma targeted therapy: insight into future of molecular approaches. Mol Cancer 2022; 21: 39.
[20] Xu S, Tang L, Li X, Fan F and Liu Z. Immunotherapy for glioma: current management and future application. Cancer Lett 2020; 476: 1-12.
[21] Pellerino A, Bruno F, Internò V, Rudà R and Soffietti R. Current clinical management of elderly patients with glioma. Expert Rev Anticancer Ther 2020; 20: 1037-1048.
[22] Gállego Pérez-Larraya J and Delattre JY. Management of elderly patients with gliomas. Oncologist 2014; 19: 1258-1267.
[23] Babu R, Komisarow JM, Agarwal VJ, Rahimpour S, Iyer A, Britt D, Karikari IO, Grossi PM, Thomas S, Friedman AH and Adamson C. Glioblastoma in the elderly: the effect of aggressive and modern therapies on survival. J Neurosurg 2016; 124: 998-1007.
[24] Luo C, Song K, Wu S, Hameed NUF, Kudulaiti N, Xu H, Qin ZY and Wu JS. The prognosis of

glioblastoma: a large, multifactorial study. Br J Neurosurg 2021; 35: 555-561.
[25] Zhang Z, Jin Z, Liu D, Zhang Y, Li C, Miao Y, Chi X, Feng J, Wang Y, Hao S and Ji N. A nomogram predicts individual prognosis in patients with newly diagnosed glioblastoma by integrating the extent of resection of non-enhancing tumors. Front Oncol 2020; 10: 598965.
[26] Carson KA, Grossman SA, Fisher JD and Shaw EG. Prognostic factors for survival in adult patients with recurrent glioma enrolled onto the new approaches to brain tumor therapy CNS consortium phase I and II clinical trials. J Clin Oncol 2007; 25: 2601-2606.
[27] Patil N, Somasundaram E, Waite KA, Lathia JD, Machtay M, Gilbert MR, Connor JR, Rubin JB, Berens ME, Buerki RA, Choi S, Sloan AE, Penas-Prado M, Ashby LS, Blumenthal DT, Werner-Wasik M, Hunter GK, Flickinger JC, Wendland MM, Panet-Raymond V, Robins HI, Pugh SL, Mehta MP and Barnholtz-Sloan JS. Independently validated sex-specific nomograms for predicting survival in patients with newly diagnosed glioblastoma: NRG Oncology RTOG 0525 and 0825. J Neurooncol 2021; 155: 363-372.
[28] Frappaz D, Bonneville-Levard A, Ricard D, Carrie S, Schiffler C, Xuan KH and Weller M. Assessment of Karnofsky (KPS) and WHO (WHO-PS) performance scores in brain tumour patients: the role of clinician bias. Support Care Cancer 2021; 29: 1883-1891.
[29] Ly KI, Wen PY and Huang RY. Imaging of central nervous system tumors based on the 2016 World Health Organization Classification. Neurol Clin 2020; 38: 95-113.
[30] Romano A, Calabria LF, Tavanti F, Minniti G, Rossi-Espagnet MC, Coppola V, Pugliese S, Guida D, Francione G, Colonnese C, Fantozzi LM and Bozzao A. Apparent diffusion coefficient obtained by magnetic resonance imaging as a prognostic marker in glioblastomas: correlation with MGMT promoter methylation status. Eur Radiol 2013; 23: 513-520.
[31] Pérez-Beteta J, Molina-García D, Martínez-González A, Henares-Molina A, Amo-Salas M, Luque B, Arregui E, Calvo M, Borrás JM, Martino J, Velásquez C, Meléndez-Asensio B, de Lope ÁR, Moreno R, Barcia JA, Asenjo B, Benavides M, Herruzo I, Lara PC, Cabrera R, Albillo D, Navarro M, Pérez-Romasanta LA, Revert A, Arana E and Pérez-García VM. Morphological MRI-based features provide pretreatment survival prediction in glioblastoma. Eur Radiol 2019; 29: 1968-1977.
[32] Butler M, Pongor L, Su YT, Xi L, Raffeld M, Quezado M, Trepel J, Aldape K, Pommier Y and Wu J. MGMT status as a clinical biomarker in glioblastoma. Trends Cancer 2020; 6: 380-391.
[33] Dahlrot RH, Dowsett J, Fosmark S, Malmström A, Henriksson R, Boldt H, de Stricker K, Sørensen MD, Poulsen HS, Lysiak M, Söderkvist P, Rosell J, Hansen S and Kristensen BW. Prognostic value of O-6-methylguanine-DNA methyltransferase (MGMT) protein expression in glioblastoma excluding nontumour cells from the analysis. Neuropathol Appl Neurobiol 2018; 44: 172-184.
[34] Pekmezci M, Rice T, Molinaro AM, Walsh KM, Decker PA, Hansen H, Sicotte H, Kollmeyer TM, McCoy LS, Sarkar G, Perry A, Giannini C, Tihan T, Berger MS, Wiemels JL, Bracci PM, Eckel-Passow JE, Lachance DH, Clarke J, Taylor JW, Luks T, Wiencke JK, Jenkins RB and Wrensch MR. Adult infiltrating gliomas with WHO 2016 integrated diagnosis: additional prognostic roles of ATRX and TERT. Acta Neuropathol 2017; 133: 1001-1016.
[35] Killela PJ, Pirozzi CJ, Healy P, Reitman ZJ, Lipp E, Rasheed BA, Yang R, Diplas BH, Wang Z, Greer PK, Zhu H, Wang CY, Carpenter AB, Friedman H, Friedman AH, Keir ST, He J, He Y, McLendon RE, Herndon JE 2nd, Yan H and Bigner DD. Mutations in IDH1, IDH2, and in the TERT promoter define clinically distinct subgroups of adult malignant gliomas. Oncotarget 2014; 5: 1515-1525.
[36] Labussière M, Boisselier B, Mokhtari K, Di Stefano AL, Rahimian A, Rossetto M, Ciccarino P, Saulnier O, Paterra R, Marie Y, Finocchiaro G and Sanson M. Combined analysis of TERT, EGFR, and IDH status defines distinct prognostic glioblastoma classes. Neurology 2014; 83: 1200-1206.
[37] Sun MZ, Oh T, Ivan ME, Clark AJ, Safaee M, Sayegh ET, Kaur G, Parsa AT and Bloch O. Survival impact of time to initiation of chemoradiotherapy after resection of newly diagnosed glioblastoma. J Neurosurg 2015; 122: 1144-1150.
[38] Zhang M, Xu F, Ni W, Qi W, Cao W, Xu C, Chen J and Gao Y. Survival impact of delaying postoperative chemoradiotherapy in newly-diagnosed glioblastoma patients. Transl Cancer Res 2020; 9: 5450-5458.
[39] Seidlitz A, Siepmann T, Löck S, Juratli T, Baumann M and Krause M. Impact of waiting time after surgery and overall time of postoperative radiochemotherapy on treatment outcome in glioblastoma multiforme. Radiat Oncol 2015; 10: 172.